Spectroscopic Properties and Ligand Field Analysis of *trans*-Dibromo(2,2-dimethyl-1,3-diaminopropane)chromium(III) Moiety

Jong-Ha Choi,* In-Gyung Oh, Woo-Taik Lim, Keon Sang Ryoo, Dong Il Kim,† and Yu Chul Park†

*Department of Chemistry, Andong National University, Andong 760-749, Korea. *E-mail: jhchoi@andong.ac.kr*
†Department of Chemistry, Kyungpook National University, Daegu 702-701, Korea
Received March 21, 2005

The sharp-line absorption and emission spectra of $(H_{13}O_6)\{trans\text{-}[Cr(Me_2tn)_2Br_2]\}_2Br_2(ClO_4)$ (Me_2tn = 2,2-dimethyl-1,3-diaminopropane) have been measured between 13000 cm^{-1} and 16000 cm^{-1} at 5 K. The 298 K infrared and visible absorption spectra have also been measured. The nine electronic bands due to spin-allowed and spin-forbidden transitions were assigned. Using observed transitions, a ligand field analysis has been performed to probe the ligand field properties of coordinated atoms in the title chromium(III) complex ion. The zero-phonon line in the sharp-line absorption spectrum splits into two components by 286 cm^{-1}, and the large ^2E_g splitting can be reproduced by the modern ligand field theory. It is confirmed that nitrogen atoms of the Me_2tn ligand have a strong σ-donor character, but the bromide has weak σ- and π-donor properties toward chromium(III) ion.

Key Words : Electronic transitions, Dibromochromium(III), Bidentate Me_2tn, AOM parameter

Introduction

The chromium(III) doped crystals are promising materials for tunable solid state laser in the near-IR spectral region.[1] As a prerequisite for these applications, a detailed study of the spectroscopic and ligand field properties is needed. In the past two decades a considerable amount of data concerning the ligand field analysis and the highly resolved optical spectra of chromium(III) complexes have been accumulated.[2-8] The sharp-line electronic spectroscopic techniques offer a promise in determining metal-ligand bonding properties and in obtaining geometric information, especially in noncrystalline environments.[9,10]

The synthesis and structural characterization of the $(H_{13}O_6)\{trans\text{-}[Cr(Me_2tn)_2Br_2]\}_2Br_2(ClO_4)$ (Scheme 1; Me_2tn = 2,2-dimethyl-1,3-diaminopropane) have been reported.[11]

However, the vibrational and electronic energy levels based on the emission and sharp-line electronic spectroscopy of this complex have not been published yet. The structures of the Me_2tn and its related bidentate ligands are shown in Figure 1.

In this study, we have measured the low-temperature absorption and emission spectra, and the room-temperature infrared spectra of $(H_{13}O_6)\{trans\text{-}[Cr(Me_2tn)_2Br_2]\}_2Br_2(ClO_4)$. The pure electronic origins due to spin-allowed and spin-forbidden transitions were assigned by analyzing the visible and sharp-line absorption spectra. Using the observed electronic transitions, a ligand field analysis has been performed to determine the detailed bonding properties for the coordinated bromide and nitrogen atoms toward chromium(III) ion.

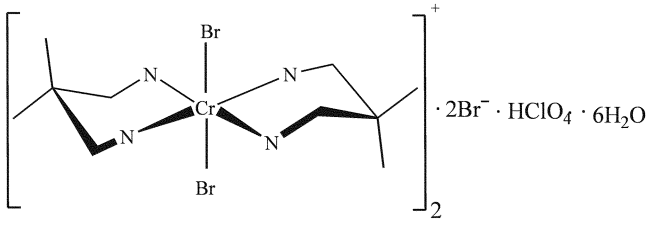

Scheme 1

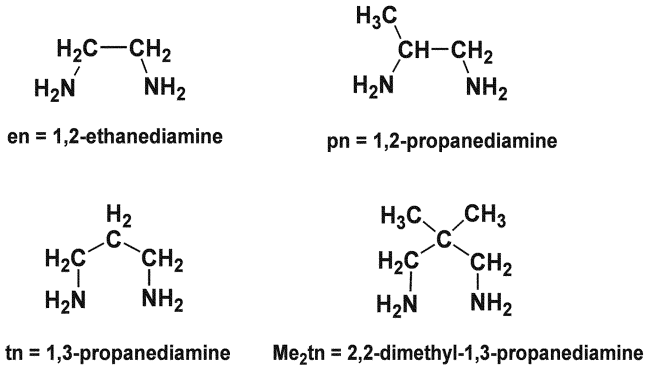

Figure 1. The structures of the Me_2tn and its related bidentate ligands.

Experimental Section

Preparations. The ligand, 2,2-dimethyl-1,3-propanediamine was purchased from Aldrich Chemical Company. All other chemicals were of reagent grade or better quality and used without further purification. The complex $(H_{13}O_6)\{trans\text{-}[Cr(Me_2tn)_2Br_2]\}_2Br_2(ClO_4)$ was prepared as described previously.[11] The compound was recrystallized three times for spectroscopic measurements.

Physical Measurements. The mid-infrared spectrum was obtained with a Mattson Infinities series FT-IR spectrometer

using a KBr pellet. The far-infrared spectrum in the region 600-50 cm^{-1} was recorded with a Bruker 113v spectrometer on a microcrystalline sample pressed into a polyethylene pellet.[4,5] The UV-visible absorption spectrum was recorded with HP 8453 diode array spectrophotometer. The sharp-line absorption spectrum was measured on a Microcrystal spectrometer.[12] Luminescence spectrum was excited by using a Spectra Physics SP375 dye laser pumped by a Spectra Physics SP171 Ar^+ laser. The luminescence was dispersed by a Spex 1404 double monochromator and detected by a RCA 31034 photomultiplier. The samples were cooled to 5 K by a helium flow-tube cryostat.

Results and Discussion

Infrared and Emission Spectra. The $[Cr(Me_2tn)_2Br_2]^+$ moiety can be exist as *trans* and *cis* geometric isomers. The infrared spectroscopy is frequently useful in elucidating structures and determining the number of functional groups involved in coordination. Two general approaches to the interpretation of the spectra are employed. The multiplicity of peaks associated with a given vibrational band has been used, with the less symmetric *cis* isomer having the greater multiplicity for a structurally sensitive band. The relative position of a peak in a certain absorption band has shown to be dependent on the structure of the complex.[13] The mid and far-infrared spectra of $(H_{13}O_6)\{$*trans*-$[Cr(Me_2tn)_2Br_2]\}_2Br_2$-$(ClO_4)$ recorded at room temperature are presented in Figures 2 and 3, respectively.

An absorption peak at 3422 cm^{-1} can easily be assigned to the O-H stretching of H_2O molecule in the hydrate complex. The strong bands in the regions of 3100-3300 cm^{-1} and 2800-3000 cm^{-1} due to the symmetric and antisymmetric N-H and C-H stretching modes, respectively. The two strong absorption bands at 1590 and 1576 cm^{-1} and the band at 1473 cm^{-1} can be assigned to NH_2 and CH_2 bending modes.[13] The splitting of the absorption band in the 1500-1600 cm^{-1} region (asymmetric NH_2 deformation) may be due to the site effect. It is well known that *cis* isomer exhibits at least three bands in the 890-830 cm^{-1} region due to the NH_2 rocking mode while the methylene vibration splits into two peaks in the 830-760 cm^{-1} region. However, *trans* isomer shows two groups of bands, one band near 890 cm^{-1} arising from the amine vibration and a doublet near 800 cm^{-1} due mainly to the methylene vibration.[14] The present complex exhibits one band at 893 cm^{-1} in the NH_2 rocking frequency region. The CH_2 rocking bands at 771 and 780 cm^{-1} are also observed. The very strong absorption at 630 cm^{-1} and strong band at 1087 cm^{-1} are assigned to ionic perchlorate.[13]

The meta-ligand stretching and ring-deformation bands occur in the far infrared range. The far-infrared spectrum (530-50 cm^{-1}) was measured in order to assign the Cr-Br and Cr-N(Me_2tn) stretching vibrations. For the *trans*-$[CrN_4Br_2]^+$ complex with D_{4h} symmetry, the group theoretical analysis predicts two Cr-N and one Cr-Br infrared-active stretching vibrations, respectively.[15] The two strong peaks at 442 and 419 cm^{-1} can be assigned to the Cr-N stretching modes. Typically, all dibromochromium(III) complexes exhibit absorption bands in the 305-285 cm^{-1} region due to the ν(M-Br).[13,15,16] The Cr-Br stretching band which we have assigned a *trans* dibromo geometric configuration exhibit no splitting, whereas the *cis* isomer shows splitting of these bands, as would be expected from the lower symmetry. The one strong absorption near 299 cm^{-1} may be due to the Cr-Br stretching mode. The *cis* isomer with an idealized C_{2v} symmetry exhibits two bands at 303 and 289 cm^{-1}.[16] The title complex was consistent with the *trans* configuration. The several absorption bands lower than 274 cm^{-1} arise from the skeletal bending and lattice vibration modes.

An experimental problem lies with the difficulty in distinguishing pure electronic components from the vibronic bands that also appear in the sharp-line spectrum. The emission spectra can be used in addition to the far-infrared spectra to extract the vibrational intervals of electronic ground state. The 5 K emission spectrum of $(H_{13}O_6)\{$*trans*-$[Cr(Me_2tn)_2Br_2]\}_2Br_2(ClO_4)$ is shown in Figure 4. The band positions relative to the lowest zero phonon line, with

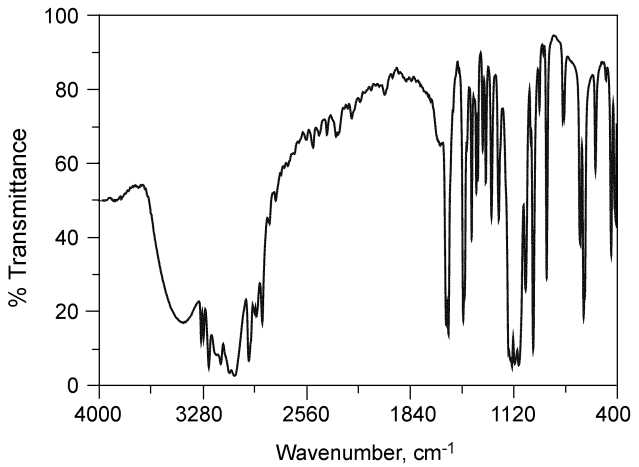

Figure 2. Mid-infrared spectrum of $(H_{13}O_6)\{$*trans*-$[Cr(Me_2tn)_2Br_2]\}_2Br_2(ClO_4)$ at 298 K.

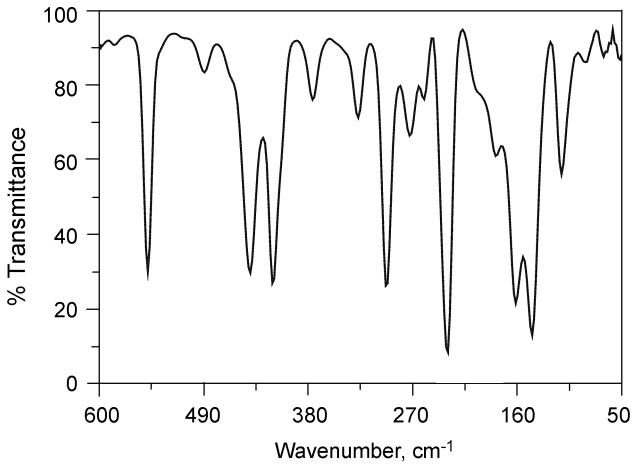

Figure 3. Far-infrared spectrum of $(H_{13}O_6)\{$*trans*-$[Cr(Me_2tn)_2Br_2]\}_2Br_2(ClO_4)$ at 298 K.

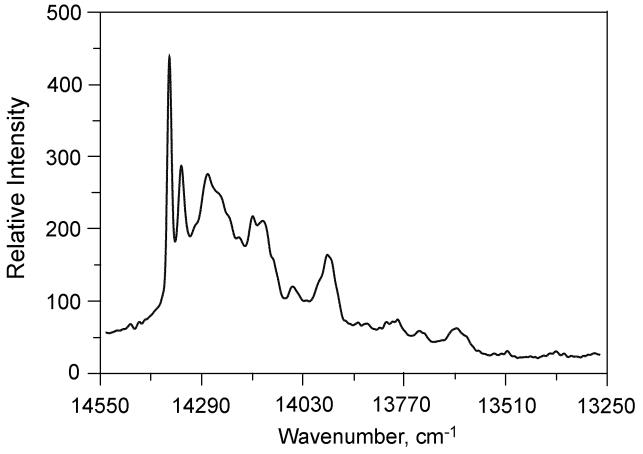

Figure 4. The emission spectrum of $(H_{13}O_6)\{trans$-$[Cr(Me_2tn)_2Br_2]\}_2Br_2(ClO_4)$ at 5 K.

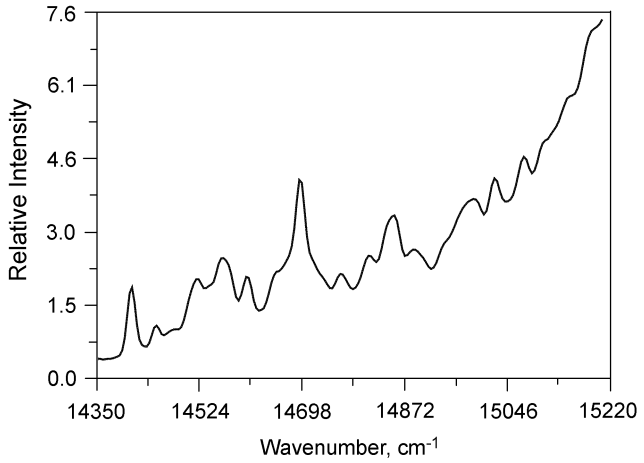

Figure 5. The sharp-line electronic absorption spectrum of $(H_{13}O_6)\{trans$-$[Cr(Me_2tn)_2Br_2]\}_2Br_2(ClO_4)$ at 5 K.

corresponding infrared frequencies, are listed in Table 1.

The very strong peak at 14374 cm^{-1} can be assigned to the zero-phonon line, R_1 because a corresponding strong peak is found at 14413 cm^{-1} in the absorption spectrum. The strong peak at 14343 cm^{-1} may be assigned to the same component (R_1') of the different site in the complex. It is conformed that the 31 cm^{-1} splitting is due to the two inequivalent sites because the structural analysis also reveals the crystal to contain two crystallographically independent chromium(III) moieties. The bands at 419 and 477 cm^{-1} can be assigned to a Cr-N stretching modes.[17-19] The vibronic intervals occurring in the spectrum consist of several modes that can be presumed to involve primarily ring torsion and angle-bending modes with frequencies in the range 250-60 cm^{-1}.

Absorption Spectra. Intraconfigurational $t_{2g}^3 \rightarrow t_{2g}^3$ transitions in chromium(III) complexes, when measured at sufficiently low temperatures, may give rise to narrow zero-phonon lines as well as a series of vibronic induced sharp-lines dues spin-forbidden transitions from the $^4A_{2g}$ ground state into the higher doublets ^2E_g, $^2T_{1g}$ and $^2T_{2g}$. The 5 K sharp-line absorption spectrum of $(H_{13}O_6)\{trans$-$[Cr(Me_2tn)_2Br_2]\}_2Br_2(ClO_4)$ is shown in Figure 5. The peak positions and their assignments are tabulated in Table 2. The calculated frequencies in parentheses were obtained by using the vibrational modes ν_1-ν_4 listed in Table 2.

Table 1. Vibrational frequencies from the 5 K Emission and 298 K infrared spectra for $(H_{13}O_6)\{trans$-$[Cr(Me_2tn)_2Br_2]\}_2Br_2(ClO_4)$[a]

Emission[b]	Infrared	Assignment
0 vs		R_1
31 s		R_1'
98 m	68 w, 89 sh	Lattice vib., skeletal bends and ν (Cr-Br)
133 sh	114 s, 145 m	
214 m	183 vw, 214 sh	
244 m	233 vs, 258 vw, 274 w	
	299 vs	
317 w	328 m, 376 w	
419 s	419 vs, 442 vs	ν (Cr-N)
477 vw	490 vw	
506 vw		ν (Cr-N) + ring def.
562 w	550 vs	
645 w	630 vs, 659 s	ClO_4^-
743 w	770 m, 780 m	ρ (CH_2)
866 w		
891 w	893 vs	ρ (NH_2)

[a]Data in cm^{-1}. [b]Measured from zero-phonon line at 14374 cm^{-1}.

The two strong peaks at 14413 and 14699 cm^{-1} in the sharp-line absorption spectrum are assigned to the two components (R_1 and R_2) of the $^4A_{2g} \rightarrow {}^2E_g$ transition. The 286 cm^{-1} splitting of the ^2E_g state can be compared to the 198 cm^{-1} and 181 cm^{-1} observed for *cis*-$[Cr(trien)Cl_2]Cl$ and $[Cr(NH_3)_5(imH)](ClO_4)_3$ complexes, respectively.[20,21] The medium peak at 14457 cm^{-1} may be assigned to the same component (R_1') of the different site in the complex thus the 44 cm^{-1} splitting is due to the site effect.

In general, it is not easy to locate the positions of the other electronic components because the vibronic sidebands of the ^2E_g levels overlap with the zero phonon lines of $^2T_{1g}$. However, the three tentative components of the $^4A_{2g} \rightarrow {}^2T_{1g}$ electronic origin (T_1, T_2 and T_3) are assigned to relatively intense peaks at 580, 618 and 660 cm^{-1} from the lowest electronic line, R_1. Vibronic satellites based on these origins have similar frequencies and intensity patterns to those of the ^2E_g components. These three electronic lines are somewhat less intense than the ^2E_g lines, but they are relatively intense compared to other chromium(III) complexes.

The visible absorption spectrum (solid line) of $(H_{13}O_6)$-$\{trans$-$[Cr(Me_2tn)_2Br_2]\}_2Br_2(ClO_4)$ in aqueous solution at room temperature is also represented in Figure 6.

It exhibits main two bands, one at 16180 cm^{-1} (ν_1), and the other at 25810 cm^{-1} (ν_2), corresponding to the $^4A_{2g} \rightarrow {}^4T_{2g}$ and $^4A_{2g} \rightarrow {}^4T_{1g}$ (O_h) transitions, respectively.[22] The assignment of geometrical configuration is suggested by inspection of the d-d absorption spectra. The position of the spin-allowed transitions in the electronic spectra, the number of bands, and their coefficients are usually reliable indicators for distinguishing the *cis* and *trans* geometrical isomers. In

Table 2. Peak positions in the 5 K sharp-line absorption spectrum of $(H_{13}O_6)\{trans\text{-}[Cr(Me_2tn)_2Br_2]\}_2Br_2(ClO_4)$[a]

$\bar{\nu}_0$ -14413	Assignment	Calcd[b]		Vibronic frequencies	Ground state frequencies[c]
0 vs	R_1		ν_1	117	114
44 m	R_1'		ν_2	157	162
111 m	$R_1+\nu_1$	(117)	ν_3	252	258
160 s	$R_1+\nu_2$	(157)	ν_4	444	444
196 s	$R_1+\nu_2$	(201)			
258 w	$R_1+\nu_3$	(252)			
286 vs	R_2				
321 sh	$R_1+2\nu_1$	(314)			
358 m	$R_1'+2\nu_1$	(358)			
406 m	$R_2+\nu_1$	(403)			
444 vs	$R_1+\nu_4$	(444)			
479 m	$R_2+\nu_4$	(488)			
580 s	T_1				
618 vs	T_2				
668 s	T_3				
703 w	$T_1+\nu_1$	(697)			
739 w	$T_1+\nu_2$	(737)			
783 w	$T_3+\nu_3$	(785)			
833 sh	$T_1+\nu_2$	(832)			

[a]Data in cm^{-1}. [b]Values in parentheses represent the calculated frequencies based on the vibrational modes listed. [c]From the emission and far-infrared spectra (Table 1).

general, the less symmetrical *cis* chromium(III) complexes have two symmetric bands in the visible region, and these bands are located at lower wavelengths and have higher extinction coefficients than those of more symmetrical *trans*-isomers.[5-7, 22] The one quartet band has a shoulder peak at 21740 cm^{-1} and shows asymmetric profile. This property of the quartet band is indicative of the *trans* configuration. In order to have some point of the reference for the splitting of the bands, we have fit the band profiles to four Gaussian curves, as seen in Figure 5. The contribution from outside bands was corrected for fine deconvolution.[23] A deconvolution procedure[21] on the experimental band pattern yielded

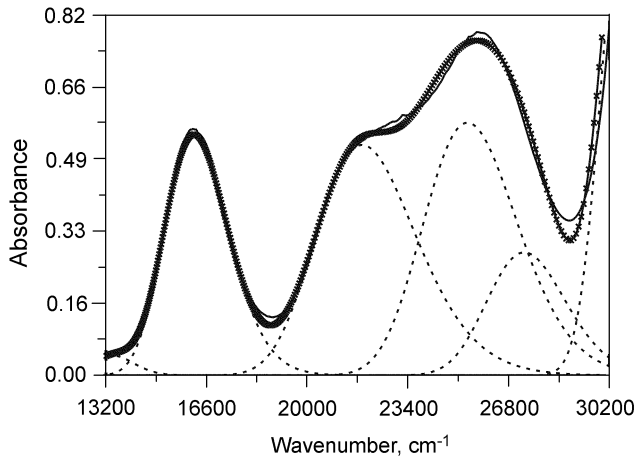

Figure 6. The visible absorption spectrum of *trans*-$[Cr(Me_2tn)_2Br_2]^+$ and the resolved overlapping peaks (dotted curves).

maxima at 16170, 21845, 25400 and 27320 cm^{-1} for the noncubic split levels of $^4T_{2g}$ and $^4T_{1g}$, respectively. These resolved peak positions were used as the observed spin-allowed transition energies in the ligand field optimization. In fact, using just one Gaussian curve instead of two yields a least squares error only four times that of the best fit (dotted line) shown in Figure 6.

AOM Calculations. All ligand field calculations are carried out using the AOMX program.[24] A full ligand field calculation on chromium(III) complexes requires the diagonalization of a 120-dimensional secular determinant which arises from the perturbated d^3 system. The ligand field potential matrix was generated for *trans*-$[Cr(Me_2tn)_2Br_2]^+$ moiety from the coordinated four nitrogen and two bromide atoms. In the framework of the angular overlap model the metal-ligand interactions are described in terms of localized bonding parameters of σ- and π-type. The parameters varied during the optimization were the interelectronic repulsion parameters B, C and the Trees correction parameter τ, the spin-orbit coupling parameter ζ, the AOM parameters e_σ(Br) and e_π(Br) for the bromide-chromium, and e_σ(N) for the Me_2tn nitrogen-chromium. The π-interaction of the amine nitrogen with sp^3 hybridization in the Me_2tn was assumed to be negligible. However, it is noteworthy that the peptide nitrogen with sp^2 hybridization has a weak π-donor character.[25-28] Schmidtke's π-expansion parameter τ were also included in the treatment of the interelectronic repulsion term.[3] In Schmidtke's approximation, the electrostatic terms are modified by a factor τ for each constituent metal wavefunction that overlaps with a ligand π-orbital. The π-orbital expansion parameter, τ was optimized at the value 0.9892. Racah parameters depend on the value of Trees parameter a_T, which was included in the calculations.[29] For calculating minor doublet splitting, the effect of the spin-orbit coupling may become important and has to be considered then by introducing an additional parameter ζ. The angular positions of the ligating six atoms were taken from the X-ray crystal structure[11] of $(H_{13}O_6)\{trans\text{-}[Cr(Me_2tn)_2Br_2]\}_2Br_2(ClO_4)$, which was determined to be the space group *C2/m* of the monoclinic system with a cell of dimensions a = 22.3862(8), b = 24.7393(8), c = 8.3230(3) Å and β = 91.6240(10)°. The coordinates were then rotated so as to maximize the projections of the six-coordinated atoms on the Cartesian axes centered on the chromium. The resulting Cartesian and spherical coordinates for the *trans*-$[Cr(Me_2tn)_2Br_2]^+$ moiety are listed in Table 3.

The ligand field analysis was carried out through an optimized fit of experimental to calculated transition energies as follows. Since the Racah parameters influence the low-symmetry level splitting only by high order perturbation, these quantities can be determined in good approximation from the quartet band separation ($^4T_{1g}$ - $^4T_{2g} \approx 12B$) and from the energy position of lowest doublet term (^2E_g - $^4A_{2g} \approx 9B + 3C$). Moreover, AOM parameters should be transferable between similar compounds, leading to a value close to 7300 cm^{-1} for e_σ(N) parameter.[2-8] All parameters, except e_σ(Br) and e_π(Br), were constrained to reasonable

Table 3. Optimized Cartesian and spherical polar coordinates for ligating atoms in *trans*-[Cr(Me$_2$tn)$_2$Br$_2$]$^+$ moiety[a]

Atom[b]	*x*	*y*	*z*	θ	ϕ
N_{11}	−0.0267	−2.0781	0.0108	89.70	−90.74
N_{12}	2.0824	0.0285	0.0042	89.88	0.78
N_{11}^i	0.0267	2.0781	−0.0109	90.30	89.26
N_{12}^i	−2.0868	−0.0248	−0.0078	90.21	−179.32
Br_{11}	0.0050	−0.0091	2.4878	0.24	−61.21
Br_{11}^i	−0.0050	0.0090	−2.4879	179.76	119.06

[a]Cartesian coordinates in Å, polar coordinates in degrees. [b]Atomic labeling was adopted from Ref. 11.

limits based on the data from the other chromium(III) complexes. The six parameters were used to fit ten experimental energies: the five $^4A_{2g} \rightarrow \{^2E_g, {}^2T_{1g}\}$ components, identified in Table 4, the four $^4A_{2g} \rightarrow \{^4T_{2g}, {}^4T_{1g}\}$ components, and the splitting of the ^2E_g state. The Powell parallel subspace optimization procedure[30] was used to find the global minimum. The optimization was repeated several times with the different sets of starting parameters to verify that the same global minimum was found. The results of the optimization and the parameter set used to generate the best-fit energies are also listed in Table 4. The error margins reported for the best-fit parameters in Table 4 are based only on the propagation of the assumed uncertainties in the observed peak positions.[31] The quartet terms were given a very low weight to reflect the very large uncertainty in their position.

The deduced ligand field parameters are e_σ(N) = 7404 ± 23; e_σ(Br) = 4879 ± 48; e_π(Br) = 797 ± 16; B = 771 ± 9; C = 3115 ± 29; α_T = 200 ± 10 and z = 149 ± 45 cm^{-1}. The AOM parameters are plausible and reproduce the spectrum pretty well. The e_σ(N) value for amine nitrogen is located in the normal range.[32-37] A ligand field analysis of the sharp-line absorption and broad-band absorption spectra indicates that the bromide is a weak σ- and π-donor. The value of 7404 cm^{-1} for e_σ(N) is comparable to values for the other amines.[17-19] It is suggested that the four nitrogen atoms of the bidentate Me$_2$tn ligand have strong σ-donor properties toward chromium(III). An orbital population analysis yields a configuration of $(xy)^{1.000}(xz)^{0.972}(yz)^{0.942}(x^2\text{-}y^2)^{0.017}(z^2)^{0.069}$ for the lowest component of the ^2E_g state. The relative *d*-orbital ordering from the calculation is $E(xy)$ = 8.3 cm^{-1} < $E(xz)$ = 1593 cm^{-1} < $E(yz)$ = 1595 cm^{-1} < $E(x^2\text{-}y^2)$ = 17167 cm^{-1} < $E(z^2)$ = 22198 cm^{-1}. The value of Racah parameter, B is about 84% of the value for a free chromium(III) ion in the gas phase. These factors plus AOM parameters can be used in determining the photolabilized ligand of the photoreaction in the chromium(III) complexes and predicting the relative efficiency of the 3d-4f energy transfer in the heterometal dinuclear complexes.[38,39] The 286 cm^{-1} of observed ^2E_g splitting in the sharp-line absorption spectrum is slightly larger than the 210 and 239 cm^{-1} of *trans*-[Cr(en)$_2$Cl$_2$]Cl and *trans*-[Cr(tn)$_2$Cl$_2$]ClO$_4$, respectively.[40] It is shown that the large ^2E_g splitting can be reproduced by the modern ligand field theory. The parameter values reported here appear to be significant, as deduced on the basis of the manifold of sharp line transitions in which were obtained from the well resolved absorption spectra. The infrared and electronic spectral properties of this complex are in good agreement with the result[11] of X-ray crystallography, which show that the Cr atom is an octahedral environment coordinated by two bidentate 2,2-dimethyl-1,3-diaminopropanes and two Br atoms in a *trans* positions.

Table 4. Experimental and calculated electronic transition energies for *trans*-[Cr(Me$_2$tn)$_2$Br$_2$]$^+$ moiety[a]

State (O_h)	Exptl	Calcd[b]
^2E_g	14413	14407
	14699	14696
$^2T_{1g}$	14993	14937
	15031	15109
	15081	15179
$^4T_{2g}$	16170[c]	16221
	21845[c]	21966
$^4T_{1g}$	25400[c]	24697
	27320[c]	27202

[a]Data in cm^{-1}. [b]e_σ(N) = 7404 ± 23; e_σ(Br) = 4879 ± 48; e_π(Br) = 797 ± 16; B = 771 ± 9; C = 3115 ± 29; α_T = 200 ± 10; ζ = 149 ± 45. [c]Obtained from the Gaussian component deconvolution.

Acknowledgement. We should like to thank Prof. E. Krausz for use of his microcrystal spectrometer at Australian National University. We also thank Dr. Lesley Debono for assistance with recording the low-temperature absorption and emission spectra.

References

1. Powell, R. C. *Physics of Solid-State Laser Materials,* Springer-Verlag, New York, 1998.
2. Hoggard, P. E. *Top. Curr. Chem.* **1994**, *171*, 114.
3. Schönherr, T. *Top. Curr. Chem.* **1997**, *191*, 87.
4. Choi, J. H. *Spectrochim. Acta* **2000**, *56A*, 1653.
5. Choi, J. H. *Chem. Phys.* **2000**, *256*, 29.
6. Choi, J. H.; Oh, I. G.; Linder, R.; Schönherr, T. *Chem. Phys.* **2004**, *297*, 7
7. Choi, J. H.; Oh, I. G.; Suzuki, T.; Kaizaki, S. *J. Mol. Struct.* **2004**, *694*, 39.
8. Hoggard, P. E. *Struct. & Bonding,* **2004**, *106*, 37.
9. Hoggard, P. E. *Coord. Chem. Rev.* **1986**, *70*, 85.
10. Choi, J. H. *Bull. Korean Chem. Soc.* **1994**, *15*, 145.
11. Choi, J. H.; Suzuki, T.; Kaizaki, S. *Acta Cryst.* **2002**, *C58*, m1.
12. Krausz, E. *Aust. J. Chem.* **1993**, *46*, 1041.
13. Nakamoto, K. *Infrared and Raman Spectra of Inorganic and Coordination Compounds, Part B;* 5th Ed., John Wiley & Sons: New York, 1997.
14. Poon, C. K.; Pun, K. C. *Inorg. Chem.* **1980**, *19*, 568.
15. Hughes, M. N.; McWhinnie, W. R. *J. Chem. Soc. A* **1967**, 592.
16. Choi, J. H. *J. Photosci.* **1997**, *4*, 127.
17. Choi, J. H. *Bull. Korean Chem. Soc.* **1993**, *14*, 118.
18. Choi, J. H.; Oh, I. G. *Bull. Korean Chem. Soc.* **1993**, *14*, 348.
19. Choi, J. H. *Bull. Korean Chem. Soc.* **1997**, *18*, 819.
20. Choi, J. H. *Bull. Korean Chem. Soc.* **1998**, *19*, 575.
21. Choi, J. H. *Bull. Korean Chem. Soc.* **1999**, *20*, 81.
22. Lever, A. B. P. *Inorganic Electronic Spectroscopy*; 2nd Ed.,

Elsevier: Amsterdam, 1984.
23. *GRAMS/32 V.5.21*, Galactic Industries Corporation, Salem, NH 03079, USA, 1999.
24. Adamsky, H. *AOMX program*, Univ. of Düsseldorf, Germany, 1996.
25. Choi, J. H.; Hoggard, P. E. *Polyhedron* **1992**, *11*, 2399.
26. Choi, J. H. *Bull. Korean Chem. Soc.* **1999**, *20*, 436.
27. Choi, J. H.; Hong, Y. P.; Park, Y. C. *J. Korean Chem. Soc.* **2001**, *45*, 436.
28. Choi, J. H. *J. Photosci.* **2002**, *9*, 51.
29. Choi, J. H.; Hong, Y. P.; Park, Y. C. *Spectrochim. Acta* **2002**, *58A*, 1599.
30. Trees, R. E. *Phys. Rev.* **1951**, *83*, 756.
31. Kuester, J. L.; Mize, J. H. *Optimization Techniques with Fortran*; McGraw-Hill: New York, 1973.
32. Clifford, A. A. *Multivariate Error Analysis*; Wiley-Hasted: New York, 1973.
33. Choi, J. H. *J. Korean Chem. Soc.* **1995**, *39*, 501.